Journal of Computer-Aided Materials Design, **5:** 61–71, 1998.
KLUWER/ESCOM

First-principles study of static nanoscale friction between MoO_3 and MoS_2

GREG S. SMITH*, NORMAND A. MODINE, UMESH V. WAGHMARE and EFTHIMIOS KAXIRAS
Department of Physics, Harvard University, Cambridge, MA 02138, U.S.A.

Received 17 February 1998; Accepted 6 April 1998

Abstract. The motion of a nanoscale MoO_3 crystal on an MoS_2 substrate is an ideal case for the study of the effects of microstructure on macroscopic phenomena like friction, because both components of this system can be prepared with atomically flat surfaces. We apply a recently developed real-space density functional theory method to investigate the energetics of sliding an MoO_3 crystal on an MoS_2 substrate. We then link the results to simple models based on continuum elastic theory, in order to study the mechanical behavior of the oxide crystals under loads that correspond to realistic situations. Based on these results, we extract estimates of the force which must be applied with an atomic force microscope in order to move the oxide crystal on the substrate, for different orientations of the two components.

Keywords: Density functional theory, Linear combination of atomic orbitals, Linear elasticity theory, Nanoscale friction

1. Introduction

With the invention of the atomic force microscope (AFM), scientists are now able to fabricate and manipulate nanometer-sized mechanical systems with unprecedented precision. This experimental technique has proven particularly useful in the field of nanotribology, which studies the atomic details of lubrication and friction. Computer simulations have also proven useful in understanding certain features of these nanoscale systems. The most commonly used computational technique to study the atomic behavior of nanotribology systems is molecular dynamics, based on empirical interatomic potentials [1–3]. Though this technique has the advantage of being able to study large systems, it neglects quantum effects at the interface, and cannot naturally handle charge transfer in systems with atoms that have disparate electronegativities.

Computational approaches based on quantum mechanical formulations such as density functional theory (DFT) [4,5] have a different set of strengths. DFT calculations are parameter-free, and have produced consistently reliable results for complex systems, even in situations where the interactions cannot be described in terms of the standard paradigms (such as metallic, covalent, ionic, or van der Waals). Generally, DFT calculations are restricted to small systems, but improved computational methods and faster computers are increasing the range of systems to which these calculations can be applied. Here we use our recently developed method, ACRES [6], and a variant of it employing a linear combination of atomic orbitals

Article based on an Invited Poster presented at the workshop *Multiscale Materials Prediction: Fundamentals and Industrial Applications*, MIT, Cambridge, MA, U.S.A., September 14–16, 1997.
*To whom correspondence should be addressed.

(LCAO) scheme, to study the energetics of sliding an MoO_3 crystal and an MoS_2 substrate. We then use this information as input into simple elastic models to make estimates of experimentally measurable quantities. This bears a certain resemblance in spirit to the work of Zhong and Tománek on a layer of palladium atoms on graphite [7]; however, here we examine a more complicated system, and combine our microscopic studies with a more extensive analysis using elasticity theory, in an effort to connect to experimental results.

2. Atomistic method

ACRES, and a version of it that uses an atomic orbitals basis, referred to as ACRES-LCAO, are real-space DFT methods that efficiently utilize parallel computer architectures. Details on ACRES, and test results that demonstrate its accuracy are described elsewhere [6].

In the ACRES-LCAO method, the eigenfunctions are expanded in the standard way as a superposition of atomic orbitals $\{\phi_j(\mathbf{r})\}$:

$$\psi_k(\mathbf{r}) \approx \sum_{j=1}^{n} c_{jk}\phi_j(\mathbf{r}) \tag{1}$$

The coefficients c_{jk} are determined by solving via direct diagonalization the generalized eigenvalue equation

$$\sum_{j=1}^{n} H_{ij}c_{jk} = \epsilon_k \sum_{j=1}^{n} S_{ij}c_{jk} \tag{2}$$

where H_{ij} are the matrix elements of the Kohn–Sham Hamiltonian [5] and S_{ij} are the overlap matrix elements. The resulting eigenfunctions are used to construct the density, and the procedure is repeated until self-consistency is achieved. Since the method is fully self-consistent, calculations can be performed on systems with atoms that have disparate electronegativities.

The atomic orbitals, potentials, and charge densities are all represented on the same numerical grid, which gives the method some appealing features. First, there is no restriction on the type of orbitals that can be used. Second, the potential due to the Hartree interaction together with the atomic cores can be found directly by solving Poisson's equation using a preconditioned conjugate gradient scheme. With this approach no four-center integrals need be calculated. Third, efficient parallel implementation is straightforward: calculating matrix elements simply involves each processor multiplying the parts of the overlap integral local to its memory, then doing a global sum over all the processors.

For the ACRES and ACRES-LCAO calculations of the MoO_3/MoS_2 system presented here, we use the local-density approximation for the exchange-correlation potential [8]. To approximate the effects of the core states of the atoms we use pseudopotentials that give good physical results. For the molybdenum and sulfur atoms we use the pseudopotentials of Hamann et al. [9], and for oxygen atoms we use an optimized pseudopotential [10]. We tested the molybdenum and sulfur pseudopotentials with calculations of bulk Mo and MoS_2, and tested the oxygen pseudopotential with bulk MoO_3 calculations. We obtained a lattice constant of 3.14 Å for bulk Mo (compared to the experimental value of 3.15 Å). For bulk MoS_2 and MoO_3, we fixed the ratios of the lattice constants and internal degree of freedom to experimental values, and minimized the energy as a function of a single lattice parameter. For bulk MoS_2 we obtained a lattice constant of 3.16 Å (compared to the experimental value

of 3.16 Å), and for bulk MoO_3 we obtained a value of 3.98 Å (compared to the experimental value of 3.97 Å). When used in ACRES and ACRES-LCAO, all the pseudopotentials are 'filtered' to remove Fourier components of the pseudopotentials that vary too rapidly to be represented accurately on the numerical grid [11,12]. Analogous filtering is automatically done in plane-wave codes, since pseudopotentials are represented only up to a cutoff energy. The numerical grid spacing in the ACRES and ACRES-LCAO calculations is 0.16 Å, which corresponds to an effective plane-wave energy cutoff of 110 Ry [6].

The atomic orbitals used in the ACRES-LCAO calculations are generated from the pseudopotentials with a single-atom logarithmic-grid DFT program, modified to include an additional harmonic potential $(r/r_0)^2$ that contracts the orbitals. Previous work [13–15] has suggested that contracted orbitals, rather than free-atom orbitals, produce eigenfunctions that represent more accurately the charge density of solids or clusters. The precise value of r_0 is unimportant; we used a value of about 4 Å for all three elements. Physically, the harmonic potential simulates the constraining effect of the surrounding medium on the electron cloud of the atom.

The computational advantages of this method are significant. In applications like the one presented in this paper, the ACRES-LCAO calculations using s, p, and d orbitals are an order of magnitude faster than full ACRES calculations, and use half the memory. The disadvantage is the more restrictive basis, but the localized nature of bonding in the system under consideration suggests that this is not a serious drawback.

3. Atomistic results

Experimental work on the MoO_3/MoS_2 system has been reported recently by Sheehan and Lieber (SL in the following) [16]. SL studied the interactions between the two substances by manipulating nanometer-scale oxide crystals on a sulfide substrate with an atomic force microscope. This particular system is especially well-suited to study how the atomistic properties of an interface affect macroscopic properties such as friction, because the interface is atomically flat, and the relative positions of the atoms at the interface are known. SL's method is different from the typical AFM nanotribology experiment, which measures friction between the AFM probe itself and a substrate: in the typical experimental arrangement the details of the interface geometry are uncertain.

Among the interesting effects SL discovered in their experimental studies was that the oxide crystals exhibit a large friction anisotropy: a single oxide crystal can move easily along one of the three directions corresponding to the rows formed by the sulfur atoms in the substrate, but the crystal is difficult to move in the perpendicular direction. SL observed that the anisotropy stemmed from the relationship between the lattice constants of the two materials. If correctly oriented, the oxygen atoms at the bottom of the MoO_3 crystal fit into grooves created by the rows of sulfur atoms on the surface of the hexagonal MoS_2 crystal (see Fig. 1). The bulk lattice constants are fortuitously very close to providing a perfect fit. A simple geometric argument provides a relation between the lattice parameters so that all the oxygen atoms fit precisely in the grooves in the substrate. If the orthorhombic unit cell vectors for MoO_3 in the plane of the interface have values a and c, and if the substrate atom spacing is s, then for a perfect fit one must have

$$\frac{1}{a^2} + \frac{1}{c^2} = \frac{4}{3s^2} \tag{3}$$

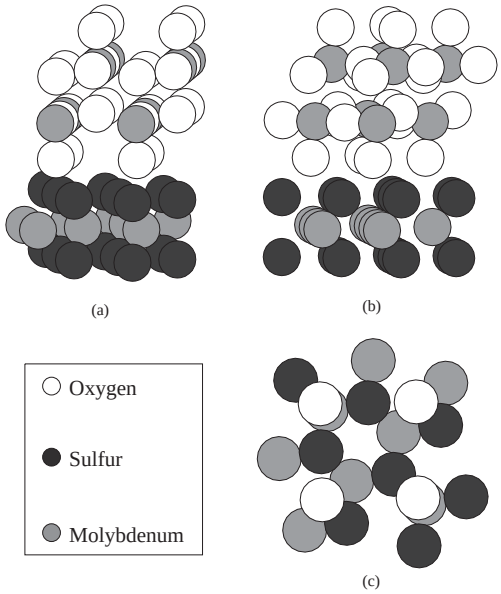

Figure 1. Views of a unit cell used in the calculations. In (a) and (b), one layer each of MoO_3 (top) and MoS_2 (bottom) is included. In (b), which is rotated about 50° with respect to (a), we show how the interface oxygen atom rows fit in the substrate grooves. (c) shows a top view of the interface, with all of the MoO_3 crystal removed except for the interface oxygen atoms.

If this expression is used to estimate c with the experimentally determined bulk values of s and a, then the estimated c deviates from the actual experimental value by 2% [17]. In the direction along the sulfur grooves, however, the oxide and sulfide crystals are incommensurate.

Due to the incommensurability along the sulfur grooves, the physical MoO_3/MoS_2 system has an extremely large unit cell, containing many hundreds of atoms. We attempt to model the system by inventing a unit cell that preserves the essential physical features, but is small enough to be computationally tractable. By distorting the bond lengths slightly we have formed a unit cell with 56 atoms that preserves the relative positioning of the atoms in each of the materials, and the geometry of the atoms at the interface. The molybdenum oxide crystal is modelled as an orthorhombic crystal with a and c both equal to 4.04 Å rather than the bulk distances of 3.97 Å and 3.70 Å, respectively; the molybdenum sulfide substrate is made up of isosceles triangles with sides of 3.19 Å (the two equal ones) and 2.87 Å instead of equilateral triangles with sides of 3.16 Å. Both MoO_3 and MoS_2 are layered materials; we include one layer each of the two substances, and 12 Å of vacuum between the free MoO_3 and MoS_2 surfaces.

To obtain a physical understanding of the nature of the interface, we examined the difference between the charge density of the isolated slabs and that of the slabs together. We did this for two configurations, one with the interface oxygen atoms on top of the sulfur atoms, and another in which they are in the grooves between the sulfur atoms. In both cases charge moves out of the interface region and into the slabs, indicating that there is no covalent bonding between the MoO_3 crystal and the MoS_2 substrate, which is consistent with the fact that both materials are layered. The local magnitude of charge depletion varies significantly throughout the region between the crystal and substrate. The charge depletion between an interface oxygen atom and a substrate sulfur atom is nearly an order of magnitude larger than the amount

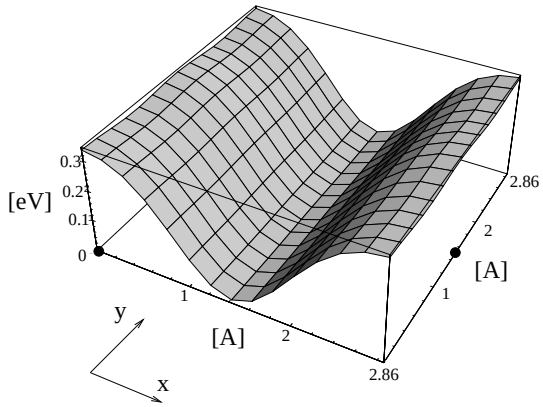

Figure 2. The fit to the energy surface. The x–y coordinates of the black dots correspond to sulfur positions; the y-axis points along the sulfur grooves. The surface is the energy of the unit cell shown in Figure 1 as a function of the position of an interface oxygen atom.

of charge depletion between an interface oxygen atom and a substrate molybdenum atom, indicating that the interaction between the former pair of atoms is primarily responsible for the behavior of the system as the two slabs move relative to each other.

We caution the reader that it is problematic to use the model unit cell adopted here in order to predict quantitatively the absolute charge depletion and transfer between the substrate and crystal in the physical system because the details of the charge movement may be sensitive to the relative distortion of the physical MoO_3 and MoS_2 unit cells. Accordingly, we rely on charge transfer calculations only to obtain order of magnitude estimates. The amount of charge depletion between an interface oxygen atom and a substrate sulfur atom is on the order of a tenth of an electron. Also, there is a charge transfer of a few tenths of an electron per model unit cell from the MoS_2 substrate to the MoO_3 crystal. The transferred charge moves from the top layer of sulfur atoms in the substrate to the interface oxygen atoms and, to a lesser extent, to the layer of oxygen and molybdenum atoms directly above in the crystal.

To determine the energetics of the interface, we studied the total energy of the system as a function of relative position of the two slabs. For each lateral relative position we found the optimal distance between the slabs by minimizing the energy. We did not include internal relaxation of the slabs. Mapping the entire energy surface is computationally intensive, so we used ACRES-LCAO whenever possible. We computed the minimized energy for 16 lateral positions using the ACRES-LCAO method to determine the shape of the energy surface shown in Fig. 2. At selected points chosen to determine the maximum energy variation along and perpendicular to the groove, we performed full ACRES calculations. As suspected by SL, the groove in the energy surface corresponds to having the O atoms of the MoO_3 slab in the channels formed between S atoms of the MoS_2 slab; the maximum energy occurs when the O atoms are on top of the S atoms. The relaxed separation between slabs shows exactly the same behavior, with a total variation of 0.5 Å from the minimum (O atoms in S grooves) to the maximum (O atoms on top of S atoms). For motion along the grooves, the variation is much less pronounced, with an amplitude of 0.01 Å.

4. Continuum analysis

Now we use the energy surface for the model MoO_3/MoS_2 system as input into continuum models, and estimate the forces required to push an oxide crystal along and perpendicular to the sulfur grooves, for various geometries. Where experimental measurements are available, we compare the calculated and measured values.

4.1. Sliding an oxide plate along the sulfur grooves

Using the energy surface in Fig. 2, we can find an upper bound for the force required to slide the oxide crystal along the direction of the sulfur grooves. Consider first a simple system consisting of two rigid commensurate lattices separated by an atomically flat interface, sliding on top of one another at zero temperature. Suppose the system begins at an energy minimum, and an external force is used to slowly slide one lattice with respect to the other until the system just reaches an energy maximum; when pushed just beyond the maximum, the system slips down irreversibly into the next energy minimum. If the average relative velocity of the two lattices is vanishingly small, then all the work done to move the system from an energy minimum to an energy maximum will be dissipated by the irreversible slip [7]. The model unit cell for the MoO_3/MoS_2 system is commensurate along the direction of the sulfur grooves, and from the magnitude of the energy variations along the groove in the energy surface in Fig. 2, we find that for the model system the average force required to slide one crystal past the other at vanishing velocity is approximately $10^{-4}A$ eV/Å, where A is the area of the interface in Å^2. However, the physical MoO_3/MoS_2 system is not rigid and not commensurate along the direction of the sulfur grooves, so this value is an upper bound. This is because in the physical system when the MoO_3 crystal is moved slightly, only some regions will slip. The regions that do slip will not settle fully into their local minima, since these regions interact elastically with other regions that have not slipped. Thus, in general, not all the work put into the system to induce slip can be dissipated[1]. Experimentally, the force to slide an MoO_3 crystal along the sulfur grooves [16] is lower than our upper bound estimate by an order of magnitude.

4.2. Pushing an oxide plate perpendicular to the sulfur grooves

We can also use the energy surface in Fig. 2 to estimate the critical force for pushing the MoO_3 crystal out of the grooves. First consider the case that the oxide crystal and sulfide substrate do not deform under the action of the AFM (i.e. are rigid bodies). Since the system is commensurate in this direction, if no torque is applied then the critical force F_{cr} is simply the force required to push an interface oxygen atom up the steepest part of the energy surface, times the number of interface oxygen atoms. Using our energy surface we find that $F_{cr} \approx 0.007A$ eV/Å where A is the area of the interface. A typically sized plate used in experiments is 1000 Å by 1000 Å, which gives a critical force of 7×10^3 eV/Å.

[1] Letting the four interface oxygen atoms in the model unit cell relax independently would not affect the validity of the upper bound estimate. When the interface oxygen atoms are in the sulfur grooves, all four of the interface oxygen atoms have the same position relative to the substrate sulfur atoms nearest each. In particular, at the minimum energy configuration along the groove, each of the four interface oxygen atoms is equidistant from the closest pair of sulfur atoms (the oxygen atoms are a distance $s/2$ away from the sulfur atoms, where s is the substrate lattice constant); at the energy maximum each is a distance $s\sqrt{3}/4$ from the closest sulfur atom. The largest effect of letting the interface oxygen atoms relax independently would be a deflection of these atoms away from the closest sulfur atom in the high energy configuration, thus lowering the energy and *reducing* the corrugation of the energy surface along the groove, maintaining the validity of the upper bound estimate.

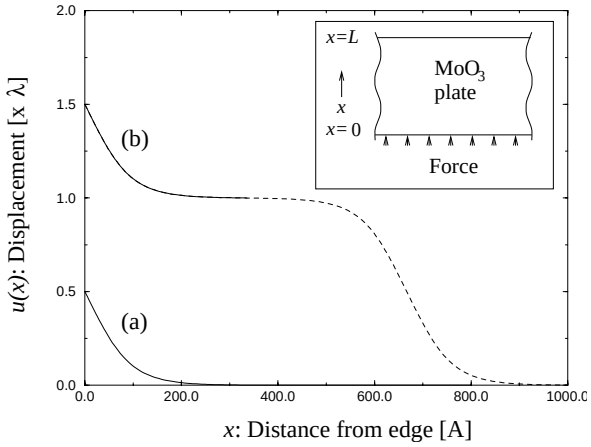

Figure 3. Numerical solutions of the displacement of an MoO_3 crystal on an MoS_2 substrate. A uniform force is applied to an edge of the oxide crystal. Curve (a) is the solution for an edge displacement of $\lambda/2$, and curve (b) is the solution for an edge displacement of $3\lambda/2$, where λ is the distance between sulfur rows. The dashed part of curve (b) can be thought of as a dislocation. The inset shows the geometry of the system.

Though critical force estimates in the infinitely stiff limit provide a useful upper bound, elastic deformation can dramatically lower the critical forces. Elastic deformation is particularly important in the MoO_3/MoS_2 system, because a localized force is applied at the edge of the sliding crystal. In contrast, in most nanotribology experiments a body force is applied to the sliding crystal. As a simple model, we include elastic effects by treating the MoO_3 crystal as a two-dimensional isotropic elastic plate, and we neglect elastic deformation in the MoS_2 substrate; we also neglect temperature effects and assume the system remains at equilibrium. Each unit area of the plate is subject to a restoring force obtained from the energy surface in Fig. 2.

First we examine an infinitely wide elastic plate of length L compressed by a uniform force applied at one edge. The force is directed perpendicular to the sulfur grooves. If the length scale of elastic deformation is much longer than the interatomic spacing, then we can coarse-grain and treat the elastic effects using a continuous deformation field, $u(x)$. The geometry is shown in the inset of Fig. 3. The equation for the displacement, $u(x)$, is [18]

$$\frac{\mathrm{d}^2u}{\mathrm{d}x^2} - \frac{1}{Eh}G(u) = 0 \tag{4}$$

where E is Young's modulus (540 GPa for MoO_3 [19]), h is the MoO_3 crystal height (15 Å is typical in experiments), and $G(u)$ is the force per unit area that quantifies the interaction between the crystal plate and substrate.

The function $G(u)$ can be obtained from the energy surface in Fig. 2. The quantity $u(0) = u_0$ is the displacement of the edge where the force is applied, and $u(L) = u_L$ is the displacement at the opposite edge. Numerical solutions to Eq. 4 are shown in Fig. 3, for the boundary conditions $u_0 = \lambda/2$ and $u_L = 0$ (curve (a)), and $u_0 = 3\lambda/2$ and $u_L = 0$ (curve (b)), where $\lambda = 2.86$ Å is the distance between sulfur rows, and L is taken to be 1000 Å, a typical crystal size. From Fig. 3, the length scale of the decay of the displacement for the MoO_3/MoS_2 system, μ_{compress}, is approximately 100 Å. This is the distance over which the oxygen atoms relax from a position on top of the sulfur rows (as they are in both solutions in Fig. 3 at $x = 0$), to a low energy position in between the sulfur rows (the flat regions in Fig.

3). Since $\mu_{\text{compress}} \gg \lambda$, the approximation of treating the elastic properties of the MoO_3 plate on a coarse-grained, continuum scale is justified.

The solution to Eq. 4 for any u_0 and any smoothly oscillating $G(u)$ exhibits the stepwise decay to $u = 0$ seen in Fig. 3, provided that L is sufficiently large. Take, for example, a simplified $G(u) = k \sin(2\pi u/\lambda)$. Integrating Eq. 4 twice, and focusing on the decaying solution for $u(x)$ gives

$$\int_{u_0}^{u(x)} \mathrm{d}z \left[2\sin^2\left(\frac{\pi z}{\lambda}\right) + \frac{\pi Eh}{k\lambda}\left(\frac{\mathrm{d}u}{\mathrm{d}x}\right)^2 \Bigg|_L \right]^{-1/2} = -\left(\frac{k\lambda}{\pi Eh}\right)^{1/2} x \tag{5}$$

Take L to be very large[2]. Except when the integration region is very close to a zero of $G(u)$, the second term is negligible, and the solution to Eq. 5 is a displacement that decays to a zero of $G(u)$ over the length scale $\mu_{\text{compress}} = \sqrt{\lambda Eh/k}$. On the other hand, when the first term in the bracket of the integrand is negligible, the solution is a linearly varying displacement with a very small slope. Thus, if the initial displacement u_0 is on the order of several λ, then the solution $u(x)$ will decay from u_0 down to a nearby zero of $G(u)$, remain there for a distance, decay down to the next zero of $G(u)$, and so on until the displacement reaches zero.

The regions over which $u(x)$ decays from one zero of $G(u)$ to the next can be viewed as dislocations. In moving the plate edge from $\lambda/2$ to $3\lambda/2$ in Fig. 3, a dislocation is emitted, which is indicated by the dotted line in (b). The width of the dislocation core is on the order of μ_{compress}. At the center of the dislocation, the interface oxygen atoms are located on top of the sulfur rows. To one side of the center the oxygen atoms are pushed in one direction by the substrate, and on the other side the oxygen atoms are pushed in the opposite direction: the net force on the dislocation is zero, and it is free to move through the system. Once the dislocation is emitted, it makes no contribution to the reaction force of the plate against the applied force. The critical force required to push the plate across the substrate is then given by the force required to emit a dislocation.

If $L < \mu_{\text{compress}}$, then using the rigid body approximation is valid, and $F_{\text{cr}} \approx 0.007A$ eV/Å. But if $L > \mu_{\text{compress}}$, then the plate begins to slip via dislocation emission, and only a small strip of the plate at the edge where the force is applied contributes to the reaction force. Since the width of the strip is of order μ_{compress}, the critical force $F_{\text{cr}} \propto W\mu_{\text{compress}}$, where W is the dimension of the plate perpendicular to the direction of the force. For a longitudinally compressed plate the stress $\sigma_{xx} = E\frac{\mathrm{d}u}{\mathrm{d}x}$, so we can find the critical force by finding the maximum derivative of the displacement at $x = 0$. This occurs when the oxygen atoms at the edge of the plate are on top of the sulfur rows. We find $F_{\text{cr}} \approx 0.8L$ eV/Å, which for a typical oxide crystal size of 1000 Å by 1000 Å gives a critical force of $F_{\text{cr}} = 800$ eV/Å.

[2]We must have that $L/n \gg \sqrt{\lambda Eh/k}$, where n is the number of sulfur grooves by which the plate edge is displaced (i.e. $u_0 = n\lambda$). In that limit, from Eq. 5 one can show

$$\sqrt{\frac{Eh}{k\lambda}}\left(\frac{\mathrm{d}u}{\mathrm{d}x}\right)\Bigg|_L \approx \exp\left(-\frac{L}{n}\sqrt{\frac{k}{Eh\lambda}}\right) \tag{6}$$

Thus the derivative of the displacement at L is very small compared to $\sqrt{Eh/k\lambda}$.

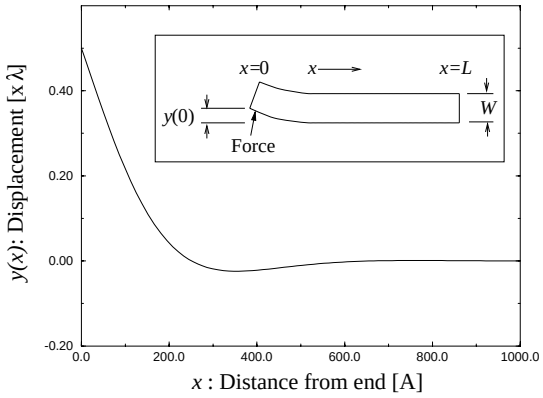

Figure 4. Numerical solution of the displacement of an MoO_3 rod 500 Å wide and 15 Å high on an MoS_2 substrate. A point force is applied at one end of the rod, displacing it by $\lambda/2$, where λ is the distance between sulfur rows. No deformation is permitted along the rod's width in this simple model. The inset shows the geometry of the system.

4.3. PUSHING AN OXIDE ROD PERPENDICULAR TO THE SULFUR GROOVES

We can also do a similar analysis for pushing an MoO_3 rod out of the substrate grooves by applying a point force at the end of the rod in a direction perpendicular to the rod's length. First consider the case where the oxide rod and substrate are rigid, and the rod is forced to pivot about a point opposite the free end where the force is applied. Then for any displacement of the free end, the force can be calculated by summing over the interface oxygen positions. Using our energy surface, we find that $F_{\mathrm{cr}} = 0.003A$ eV/Å. For a typical rod of size 500 Å by 5000 Å, this gives $F_{\mathrm{cr}} = 7.5 \times 10^3$ eV/Å.

As a simple model that incorporates elastic effects, we treat the oxide crystal as an elastic one-dimensional rod of length L. No deformation is permitted along the width of the rod. We use the same set of approximations discussed for the elastic plate model. The geometry is shown in the inset of Fig. 4. For small displacements $y(x)$ of the rod from the undistorted state [18],

$$EI\frac{\mathrm{d}^4 y}{\mathrm{d}x^4} - F(y) = 0 \tag{7}$$

where E is Young's modulus of the rod, I is the moment about the z-axis, and $F(y)$ is the restoring force per unit length obtained from the energy surface of Fig. 2. The force applied at the end will tend to bend the rod out of the grooves, while the interaction between the crystal and substrate will try to keep as much of the rod as possible in the grooves. For $y(0) \ll \lambda$, the energy surface can be approximated as a parabola so that $F(y) = -k'y$, and the solution $y(x) = \exp(-\mu_{\mathrm{bend}}x)\cos(\mu_{\mathrm{bend}}x)$, where $\mu_{\mathrm{bend}} = (k'/4EI)^{1/4}$. Using our energy surface and a typical crystal height of 15 Å, $\mu_{\mathrm{bend}} \approx 5\sqrt{W}$ Å, where W is the rod width. Physically, μ_{bend} is the length scale for small $y(0)$ over which the interface oxygen atoms have relaxed back to the center of the sulfur grooves. A numerical solution for $y(0) = \lambda/2$ using $F(y)$ obtained from the energy surface is shown in Fig. 4.

The critical force for pushing the rod out of the grooves is achieved before y_0 reaches $\lambda/2$. Once the oxygen atoms at the end of the rod are on top of or pushed over the sulfur rows, the force on these oxygen atoms due to the substrate no longer opposes the applied force, and moving oxygen atoms out of their groove further down the rod becomes increasingly easy

as the lever arm gets larger. For a slightly deflected rod, the magnitude of the applied force $F = EI\ \mathrm{d}^3y/\mathrm{d}x^3|_{x=0}$. By numerically finding the critical forces for a variety of widths and fitting, we find that $F_{\mathrm{cr}} \approx 0.03W^{3/2}$. For a typical rod of width 500 Å this gives $F_{\mathrm{cr}} \approx 3.4\times10^2$ eV/Å.

4.4. More complex models

In an experimental situation, the configuration may not be as simple as the elastic models discussed thus far. An AFM probe that pushes an MoO_3 plate applies a localized, rather than a homogeneous, force to the edge of the plate. It is reasonable that if the dimension W of the plate perpendicular to the direction of the force is not too much larger than μ_{bend}, then the dislocation will cross the crystal and remain nearly straight. The barrier will be roughly the same as in the homogeneous force case, so that $F_{\mathrm{cr}} \approx 0.8W$ eV/Å. If W is much larger than μ_{bend}, stress in the MoO_3 crystal will be concentrated near to the probe and the crystal will break. Experimentalists rely on this to machine MoO_3 crystals into desired shapes [16].

There are also complications in the case where a rod is pushed in a direction perpendicular to the direction of the grooves. If a rod is wider than μ_{compress}, then treating it as a one-dimensional object does not fully include elastic effects that lower the critical force. We speculate that if the rod width is not too much larger than μ_{compress}, then μ_{bend} continues to set the bending length of the rod. But since the rod can now deform along the width of the rod, we propose that the reaction force is supplied not by the entire width of the rod, but by a region of width μ_{compress}. Thus the critical force must be large enough to coherently move a region of interface oxygen atoms of area $\mu_{\mathrm{compress}} \times \mu_{\mathrm{bend}}$ over the substrate, which implies $F_{\mathrm{cr}} \approx 3\sqrt{W}$. For a typical rod of width 500 Å this gives $F_{\mathrm{cr}} \approx 80$ eV/Å.

5. Conclusions

In summary, we have used ACRES and ACRES-LCAO calculations to study the sliding of an MoO_3 crystal on an MoS_2 substrate. By studying a model unit cell that qualitatively reproduces the geometry of the physical system, we provided insight into the microscopic interactions between the two crystals. Using the calculated total energy as a function of relative lateral position of the two crystals, we estimated an upper bound for the force required to slide an MoO_3 crystal along the sulfur grooves, and the critical forces necessary to push the MoO_3 crystal out of the substrate grooves. The effect of incommensurability on the force needed to slide an oxide crystal parallel to the direction of the grooves, and the effects of the extreme distortion of the MoO_3 crystal caused by point forces, requires additional computational work for full quantitative understanding.

Acknowledgements

The authors gratefully acknowledge support from the Office of Naval Research Grant No. N00014-95-1-0350. Work was performed using the ACRES code developed under the CHSSI project. Calculations were performed on the CM-5 at the Naval Research Laboratory. We are indebted to P.E. Sheehan and C.M. Lieber for several helpful discussions about the MoO_3/MoS_2 system; we would also like to thank E.B. Tadmor, M.Z. Bazant, and J.R. Rice for their help with elasticity theory.

References

1. Diestler, D.J., Rajasekaran, E. and Zeng, X.C., J. Phys. Chem., B101 (1997) 4992.
2. Cieplak, M., Smith, E.D. and Robbins, M.O., Science, 265 (1994) 1209.
3. Harrison, J.A., White, C.T., Colton, R.J. and Brenner, D.W., Phys. Rev., B46 (1992) 9700.
4. Hohenberg, P. and Kohn, W., Phys. Rev., 136 (1964) B864.
5. Kohn, W. and Sham, L.J., Phys. Rev., 140 (1965) A1133.
6. Modine, N.A., Zumbach, G. and Kaxiras, E., Phys. Rev., B55 (1997) 10289.
7. Zhong, W. and Tomànek, D., Phys. Rev. Lett., 64 (1990) 3054.
8. Perdew, J. and Zunger, A., Phys. Rev., B23 (1981) 5048.
9. Hamann, D.R., Schluter, M. and Chiang, C., Phys. Rev. Lett., 43 (1979) 1494.
10. Rappe, A.M., Rabe, K.M., Kaxiras, E. and Joannopoulos, J. D., Phys. Rev., B41 (1990) 1227.
11. Briggs, E.L., Sullivan, D.J. and Bernholc, J., Phys. Rev., B54 (1996) 14362.
12. King-Smith, R.D., Payne, M.C. and Lin, J.-S., Phys. Rev., B44 (1991) 13063.
13. Eschrig, H. and Bergert, I., Phys. Status Solidi, B90 (1978) 621.
14. Porezag, D., Frauenheim, T., Köhler, T., Seifert, G. and Kaschner, R., Phys. Rev., B51 (1995) 12947.
15. Sankey, O.F. and Niklewski, D.J., Phys. Rev., B40 (1989) 3979.
16. a. Sheehan, P.E. and Lieber, C.M., Science, 272 (1996) 1158.
    b. Sheehan, P.E. and Lieber, C.M., Nanotechnology, 7 (1996) 236.
17. The question of determining in general which pairs of materials fit together well, and how precisely the materials will orient themselves relative to each other in the face of slight mismatches like in the MoO_3/MoS_2 system is discussed in Hillier, A.C. and Ward, M.D., Phys. Rev., B54 (1996) 14037.
18. Landau, L.D. and Lifshitz, E.M., Theory of Elasticity, Pergamon Press, New York, NY, 1986. Here and in the subsequent analysis, we have set Poisson's ratio to zero.
19. Hues, S.M., Draper, C.F. and Cotton, R.J., Phys. Rev., B12 (1994) 2211.